iScience

Article

Contact angle analysis of biocolonized stone surfaces: Comparative study of benchtop and portable approaches to advance on-site applications

Graphical abstract

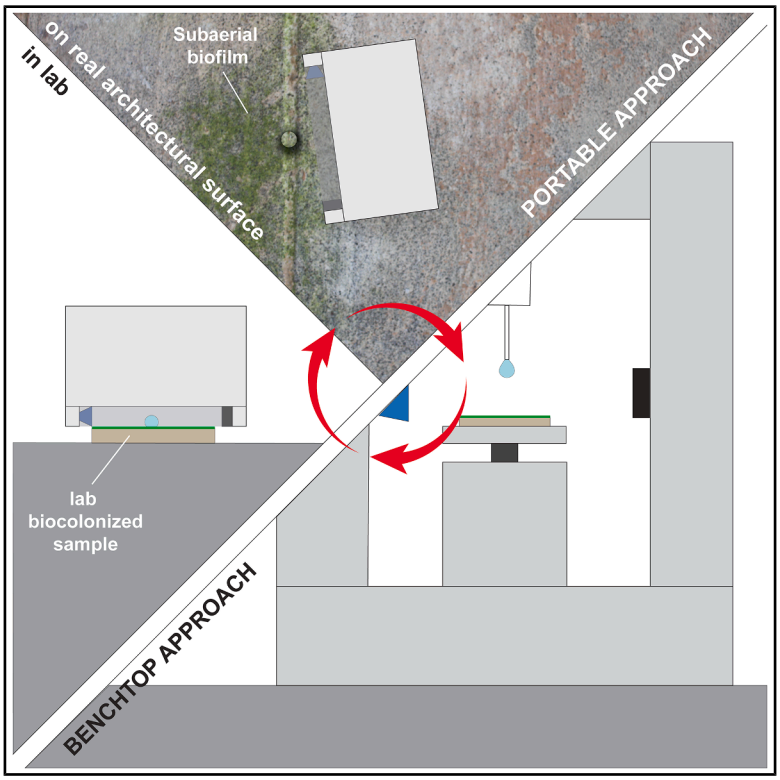

Authors

Letizia Berti, Davide Gulotta, Federica Villa, Lucia Toniolo, Gabriele Gianini, Francesca Cappitelli, Sara Goidanich

Correspondence

dgulotta@getty.edu

In brief

Chemical engineering; Chemistry; Materials science

Highlights

- WCA measurements were applied to evaluate SABs' impact on porous substrates
- A portable approach has been validated against standard benchtop methodology
- Differences in WCA behavior were found between mono- and dual-species biofilms
- The study validates a statistically robust method for on-site WCA monitoring

Berti et al., 2025, iScience *28*, 113282
September 19, 2025
https://doi.org/10.1016/j.isci.2025.113282

CellPress

iScience

CellPress
OPEN ACCESS

Article

Contact angle analysis of biocolonized stone surfaces: Comparative study of benchtop and portable approaches to advance on-site applications

Letizia Berti,[1,2,3] Davide Gulotta,[4,6,*] Federica Villa,[3] Lucia Toniolo,[2] Gabriele Gianini,[5] Francesca Cappitelli,[3] and Sara Goidanich[2]

[1]Department of Sciences of Antiquity, "La Sapienza" University of Rome, Piazzale Aldo Moro 5, 00185 Rome, Italy
[2]Department of Chemistry, Material and Chemical Engineering "Giulio Natta", Politecnico di Milano, Piazza Leonardo Da Vinci 32, 20133 Milan, Italy
[3]Department of Food, Environmental and Nutritional Sciences, Università degli Studi di Milano, Via Luigi Mangiagalli 25, 20133 Milan, Italy
[4]Getty Conservation Institute, Science Department, 1200 Getty Center Drive, Los Angeles, CA 90049, USA
[5]Department of Informatics, Systems and Communication, Università degli Studi di Milan-Bicocca, Viale Sarca 336, 20126 Milan, Italy
[6]Lead contact
*Correspondence: dgulotta@getty.edu
https://doi.org/10.1016/j.isci.2025.113282

SUMMARY

While traditionally confined to laboratory settings, recent developments have enabled Water Contact Angle (WCA) measurements to be conducted on-site, under field conditions. This study presents a comparative evaluation of a conventional benchtop method and a portable instrument applied to uncolonized and biocolonized stone surfaces. A reference non-absorbing substrate was used for method validation. Results showed good agreement between the two methods on non-absorbing surfaces, confirming the reliability of the portable approach. On porous biocolonized substrates, the methods differed in absolute WCA values but showed consistent trends, while there was good agreement among drop absorption times. These findings demonstrated that the portable approach can effectively capture water-related properties on-site, with minimal invasiveness and high reproducibility. The study introduces a validated and statistically supported methodology for on-site wettability and water absorption assessment and emphasizes the influence of biofilm composition on surface water-related properties, contributing to the broader understanding of SAB-induced surface modification.

INTRODUCTION

Weathering of building stone surfaces exposed outdoors is governed by the complex interaction between the specific substrates' properties and local environmental factors, with water playing a critical role among the latter. Liquid water is the driving force of major chemical (e.g., leaching) and physical (e.g., freeze-thaw and salt crystallization) deterioration processes.[1,2] It is also a key factor for biocolonization since microorganisms can only thrive on abiotic substrates in the presence of water in the liquid and vapor phase.[3,4] Therefore, water-related properties of built heritage materials have been extensively studied to unveil such mechanisms and, in turn, to better understand their impact on the material's durability and the performance of conservation treatments. The conventional requirements to assess the efficacy and suitability of stone surface protection treatments, for example, largely rely on measurements of water-related properties to assess changes associated with potential beneficial effects, i.e., reduced the penetration of liquid water within the porous network.

Surface wettability is a parameter that describes the affinity of a liquid droplet toward a solid phase. When the two phases are brought into contact, the resulting interface is formed upon the displacement of another fluid, usually a gaseous phase (e.g., ambient air), leading to a three-phase contact line.[5] The shape of the liquid droplet is influenced by both chemical (e.g., molecular interactions at the solid-liquid interface) and physical (e.g., surface topography, roughness) characteristics of the tested surface and of the liquid itself. On a non-wettable surface, the liquid will tend to minimize the interaction with the solid, therefore reducing the contact area. On the other hand, wettable surfaces tend to form a larger solid-liquid contact due to the higher affinity between the two phases.

Among the substrate's physical properties, surface roughness is a key parameter in defining surface wettability.[6,7] Its contribution can be expressed according to two theoretical models. In the Wenzel model, the droplet condenses to a spherical shape to avoid a large contact surface with the substrates, increased by the penetration of the liquid into the asperities (Figure S1A). According to the Cassie-Baxter one, the drop rests on top of the asperities, which become the solid-liquid-gas interface (Figure S1A). Consequently, the liquid cannot penetrate the surface roughness, and the hydrophobicity is enhanced.[5] Moreover, a transitional state between the Wenzel and the

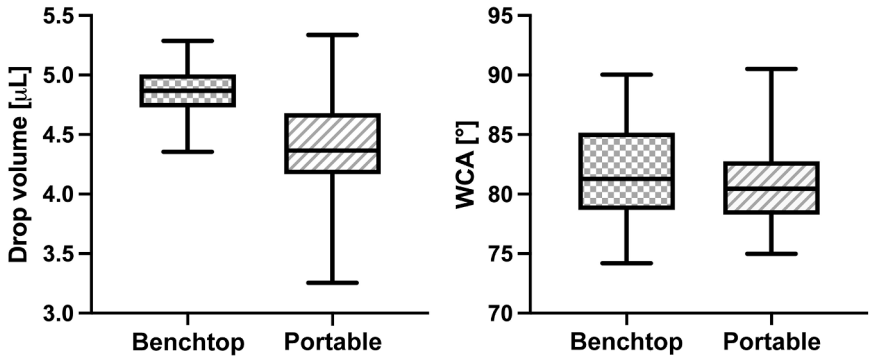

Figure 1. Drop volume and WCA values of reference polymeric surface

Drop volume [mL] and water contact angle [°] on the polymeric slab measured according to benchtop and portable measurement methods, respectively. Error bars indicate standard deviation.

Cassie-Baxter models has been described, with a partial wetting of the asperities (Figure S1A).

However, it is worth noting the mismatch between the theoretical models and real-world lithic materials, which are non-ideal surfaces with multi-scale roughness and porosity and are usually characterized by remarkable chemical heterogeneity (e.g., presence of different mineral phases).

The most used indicator of surface wettability is the Water Contact Angle (WCA). To measure it, a water drop of known volume is deposited onto the solid surface. Standard laboratory measurements rely on optical systems to acquire the water drop profile. The resulting angle formed with the substrate is then determined through image analysis.[8] The WCA is defined as the angle formed by the solid surface and the tangent to the liquid/fluid (i.e., water/air) interface at the three-phase contact point, as shown in Figure S1B. In 1805, Young[9] described the equilibrium conditions on an ideal smooth surface as follows:

$$\gamma_{SG} = \gamma_{LS} + \gamma_{LG} \cos\theta \qquad \text{(Equation 1)}$$

Where γ is the surface tension (SG, at the solid-gas interface, LS at the liquid-solid interface, and LG at the liquid-gas interface).

This equation can be simplified since the CA and the liquid surface tension can be measured:

$$\gamma = \gamma_L(\cos\theta - 1) \qquad \text{(Equation 2)}$$

From the above equation and the measured WCA, the wetting behavior of a surface can be classified. Conventionally, static contact angles are determined when the tangent to the drop at the three-phase point remains stable during the measurement, as opposed to dynamic ones when the contact line is not stationary.[8,10] Systems with static WCA of less than 90° are defined as hydrophilic, whereas those displaying WCA greater or equal to 90° are classified as hydrophobic. Superhydrophobic conditions can also be defined when 150° < WCA 180°, as well as low contact angle hysteresis and low sliding angle.[11] When considering materials of natural origin and biomaterials, which have chemical compositions and complex surface microstructures and roughness that inherently repel water,[6] some authors[12] suggested that the hydrophobicity threshold should be set for a water contact angle above 65°.[6]

Because of the non-ideal surface conditions of heterogeneous substrates, such as those investigated here, the measured static contact angle deviates from the standard definition, but the calculated value can still be considered representative of the so-called "global contact angles," according to Marmur et al. (2017),[10] i.e., an average static contact angle experimentally measured for the entire three-phase contact line. Consequently, static contact angle measurements on this type of surface often require adaptation and can only provide local partial information on the surface condition.

SubAerial Biofilms (SABs), i.e., microbial communities growing at the mineral-air interface embedded in Extracellular Polymeric Substances (EPS), have displayed the ability to alter some of the surface water-related properties of the substrates they colonized, for example, conferring hydrophobic characteristics.[13]

WCA measurement provides a powerful method for investigating surface wettability and how it may change in the presence of material of natural origin, such as SABs. However, WCA measurements still present unsolved issues when applied to biocolonized and uncolonized porous substrates, due to the dynamic evolution of the drop. In this case, SABs' adaptive behavior against external stressors is a key factor. SABs' metabolism and micro-structure change over time in response to varying environmental conditions,[14] e.g., to adapt to varying temperature and moisture regimes in the environment they are exposed to, concurrently modifying their interaction with and impact on the substrate. EPS and, in some cases, microorganisms can infiltrate porous material through different endolithic growth, making the interpretation of water-related characteristics additionally challenging.[15] It has been demonstrated that SABs' presence can reduce surface wettability and slow down water absorption, both on laboratory biocolonized samples and on real architectural surfaces.[13,14,16–18] To evaluate the wettability of biocolonized surfaces, it has been proposed to measure the WCA immediately after the drop makes contact with the surface, assuming that, at that moment, absorption is still negligible.[16–18] It could also be of interest to measure the complete drop absorption time, a parameter not fully investigated yet that can contribute to a better characterization of biocolonized surfaces and an enhanced understanding of the SABs' effects.[16,17]

Recent developments in portable instrumentation have enabled on-site WCA measurements under various conditions, including field applications to non-horizontal architectural surfaces. As a field-based alternative to conventional laboratory WCA measurements, they can provide valuable insights into the impact of SABs on the surface characteristics of porous substrates of the built environment. Moreover, they may represent a promising alternative for studying the dynamics of liquid water absorption, conventionally conducted via the contact sponge

Table 1. Drop volume and WCA values and standard deviations on polymeric slab

	Drop volume [μL]	WCA [°]
Benchtop	4.87 ± 0.19	81.79 ± 4.17
Portable	4.33 ± 0.49	80.92 ± 3.78

Drop volume [mL] and water contact angle [°] on the polymeric slab measured according to benchtop and portable measurement methods, respectively.

and Karsten tube methods, with reduced impact on the surfaces under study (i.e., reduced surface contact and water volumes required). Therefore, the potentialities of this new approach could extend beyond the sole on-site measurement of the WCA. However, this method still lacks a standardized procedure and reference datasets. Therefore, there is a need to perform a systematic investigation and comparatively assess novel portable approaches against standardized laboratory methods. In this study, for the first time, a comparison between the results obtained with a conventional laboratory benchtop instrument and a portable one is carried out. Biocolonized (based on dual-species and mono-species SABs) and uncolonized stone specimens were measured, with a non-absorbing and non-colonized polymeric surface as reference material.

This work aims to validate a portable approach to WCA analysis against a standard, laboratory-based method and to develop a statistically robust methodology for on-site WCA measurements. The minimum number of measurements required to achieve a target statistical precision was determined on a reference polymeric substrate, for both WCA values and drop volume data, providing a robust baseline for evaluating measurement reliability. Additionally, the study presents some of the first combined measurements of WCA and drop absorption time on porous, biocolonized mineral substrates by integrating the variables of biofilm microbial community composition. While further investigation is needed for a comprehensive validation of the method on a broader range of materials and environmental conditions, the results, supported by the statistical data elaboration, indicate that the portable approach can be effectively applied to investigate surface wettability properties and water absorption dynamics on-site, under outdoor conditions. These results have relevant implications for the non-destructive characterization of building material surfaces, assessing the impact of bio-colonization, and monitoring the performance of surface treatments, including conservation treatments in the built heritage preservation sector.

RESULTS AND DISCUSSION

Benchtop and portable measurements on the reference polymeric surface

Drop volume and water contact angle results

Figure 1 and Table 1 report the results of the drop volume and the static water contact angle measurements obtained on the polymeric non-absorbing reference surface. The benchtop method showed higher accuracy and reproducibility in the drop volume compared to the portable one, for which a greater dispersion of the results was observed. It must be emphasized that although the difference in the reported drop volume for the latter was statistically significant ($p < 0.0001$), the variability range was extremely limited, with mean values differing by 0.5 μL only. On the other hand, the water contact angle data between the two methods were comparable and showed non-statistically significant differences ($p = 0.3$). Therefore, the observed relatively small difference in the drop volume for the portable method apparently did not significantly affect the WCA value measured on non-absorbing surfaces. However, the drop volume may influence the absorption time of porous substrates. At present, the measurement of the drop absorption time is not yet a well-established procedure and still needs to be optimized both in terms of setup and result interpretation.[16,17,19] As previously mentioned, it could become a key parameter for investigating the protective role of SABs and the impact of conservation treatments on porous substrates.

Due to the specific dosing configuration, i.e., pressurized drop ejection units, the portable instrument can perform on-site wettability measurements with different orientations. Figure 2 shows the results obtained by the portable measurements approach with 50 drops of 5 μL on the reference surface in a horizontal and vertical orientation. They indicated that WCA values are not affected by the surface orientation. It can be noted that the surface orientation has only a slight influence on the drop volume results, with no statistically significant difference; in this case, the results are more consistent for vertical surfaces. The water droplets are sprayed through a dosing system onto the surface, making contact with it in a comparable way regardless

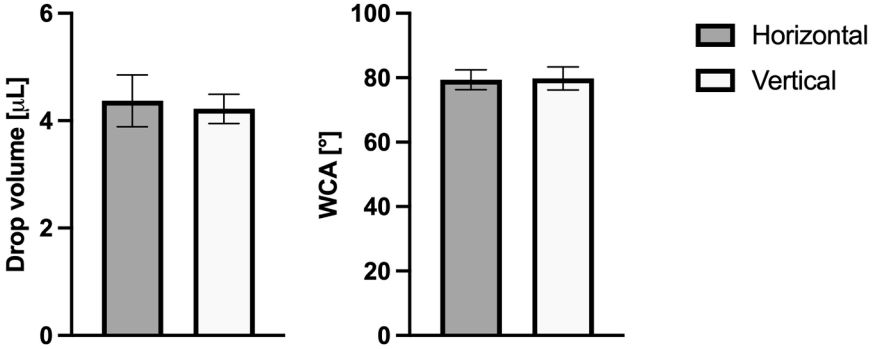

Figure 2. Effect of surface orientation on the portable approach

Drop volume [mL] and water contact angle [°] measured using the portable instrument on the plastic slab by orienting the surface horizontally and vertically. Error bars indicate standard deviation.

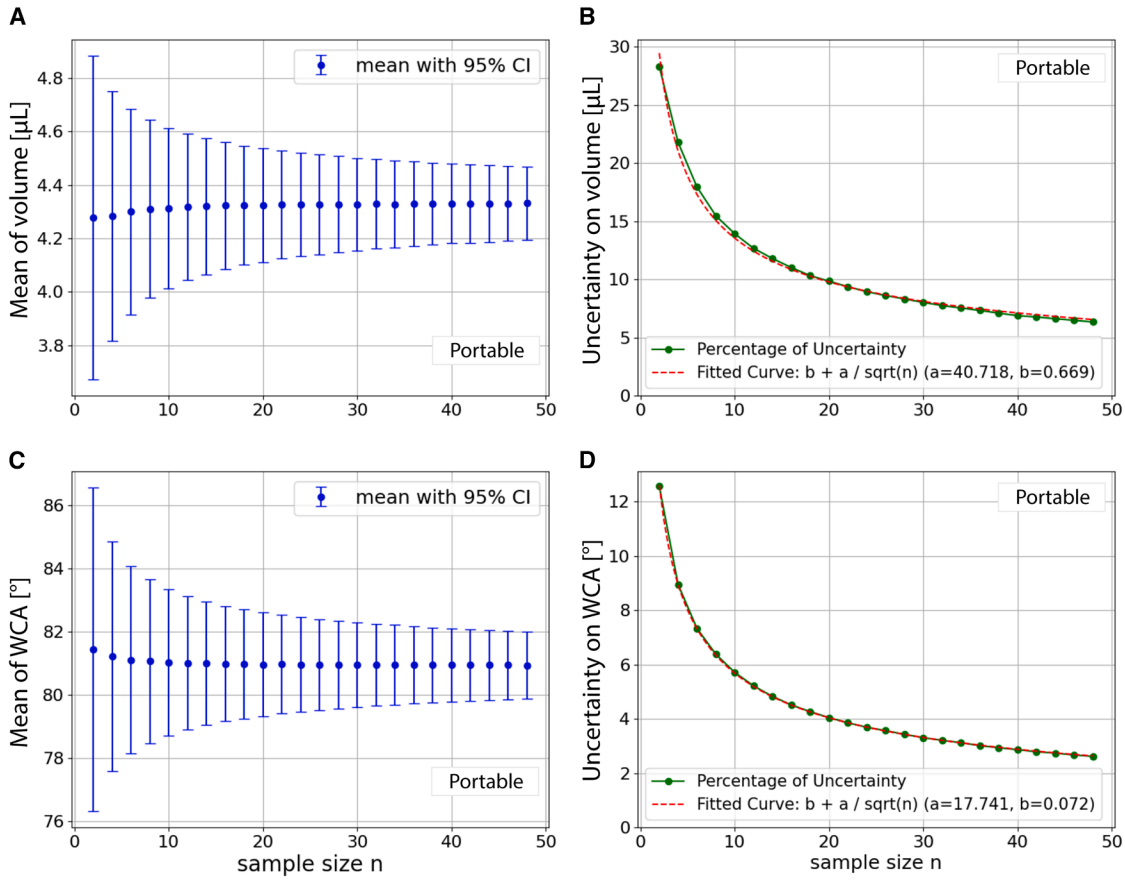

Figure 3. Sample size impact on the portable measurement method

Dependence of the 95% confidence interval on the sample sizes of (A) volume and (C) water contact angle and (B and D) the respective dependence of the percentage error implied by the confidence interval on the sample size.

of the instrument's orientation. Possible gravity effects seem negligible according to the results, likely due to the small distance between the dosing unit and the surface (a few millimeters) and the small drop volume. Overall, the results showed that working under different surface orientations does not significantly affect the reliability of the measurements.

This experimental approach enabled the evaluation of the reliability of the portable instrument in a simplified scenario where substrate-related variables are minimized. The agreement and consistency observed between the two methods on the polymeric reference material suggest that, under similar smooth and non-absorbing surface conditions, the portable and benchtop methods can provide comparable WCA results.

Variability assessment and sample size

Collecting 50 measurement values may not be feasible during on-site investigation on real architectural substrates because it is time-consuming, particularly if the complete drop absorption time is also assessed.[16,17,19] Thus, it is necessary for practical applications to define an appropriate sample size for the robust evaluation of the drop volume, WCA, and drop absorption time.

One of the aims of this study was to determine the minimum number of measurements necessary to represent the mean drop volume and WCA values reliably. The results of the bootstrap analysis for sample size determination for the portable method are illustrated in Figure 3. Figure 4 shows the comparison between portable and benchtop approaches. Figure 3A shows the 95% confidence interval as a function of the bootstrap sample size for the volume measurements. Figure 3B shows the dependence of the relative uncertainty (confidence interval of the mean over mean) on the sample size. Such dependence has been fitted with the inverse square root of n function $p(n) = b + a/\sqrt{n}$. The curve accurately fits the data. The resulting fitted parameters are a = 40.72 and b = 0.67. The inverse of the fitted function can be used to estimate the sample size necessary to achieve a predetermined precision: $n = \lceil [a/(p - b)]^2 \rceil$. For instance, to get a 10% uncertainty for the drop volume, one should collect 20 samples. The same procedure has been applied to the 50 WCA samples from the portable method. The results are shown in Figures 3B and 3C. In this case, as well, the one curve accurately fits the data. The resulting fitted parameters are a = 17.74 and b = 0.07. Using the inverse of the fitted function to estimate the sample size necessary to achieve a predetermined percentage uncertainty, we get, for instance, that to attain a target of 5% precision, one should collect 14 samples.

We carried out a similar study, based on bootstrap and regression, for the volume and WCA measurements performed with the

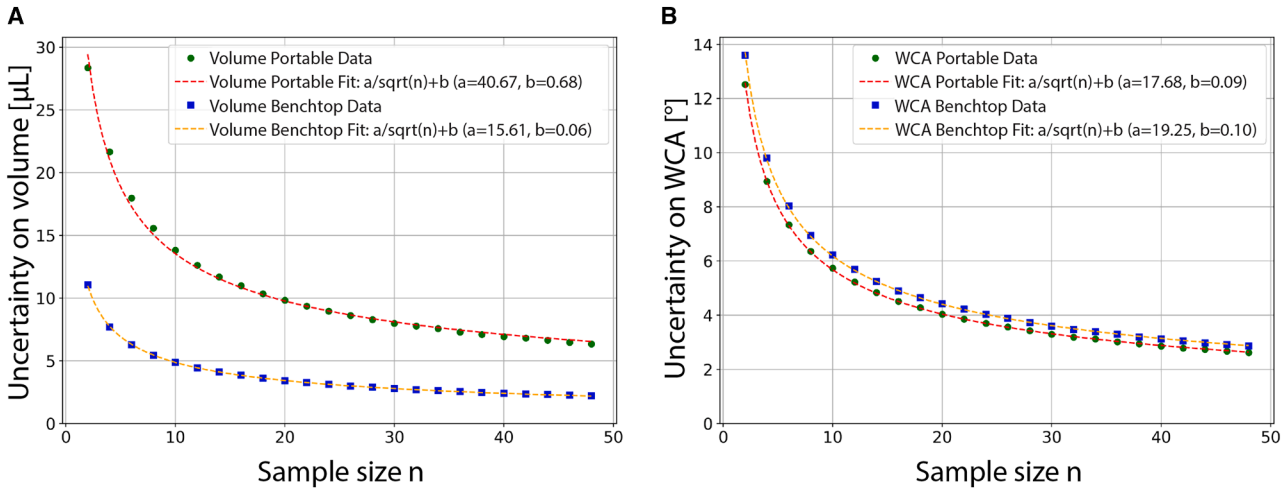

Figure 4. Uncertainty comparison between the two methods

Comparison of portable and benchtop measurement methods in terms of the relative uncertainty (95% confidence interval of the mean over mean) for (A) volume and (B) WCA.

benchtop instrument. The curve accurately fits the data in both cases: the resulting parameters for volume are a = 15.31, b = 0.01, whereas for WCA are 19.57, b = 0.04. The curves are compared in Figure 4. One can see that, for volume (Figure 4A), the uncertainty is higher with the portable instrument than with the benchtop one, given the same number of samples. For instance, with 20 samples, the volume relative uncertainty measured with the portable instrument is 9.8%, whereas the volume relative uncertainty measured with the benchtop one is about 3.4%. For WCA (Figure 4B), on the other hand, uncertainty is consistently lower with the portable measurement method than with the benchtop one, but the differences are minimal. For example, with 20 bootstrap samples, the WCA relative uncertainty with the portable instrument is 4.0, whereas the relative uncertainty is 4.4% for WCA measured with the benchtop instrument. These findings are consistent with those implied by the

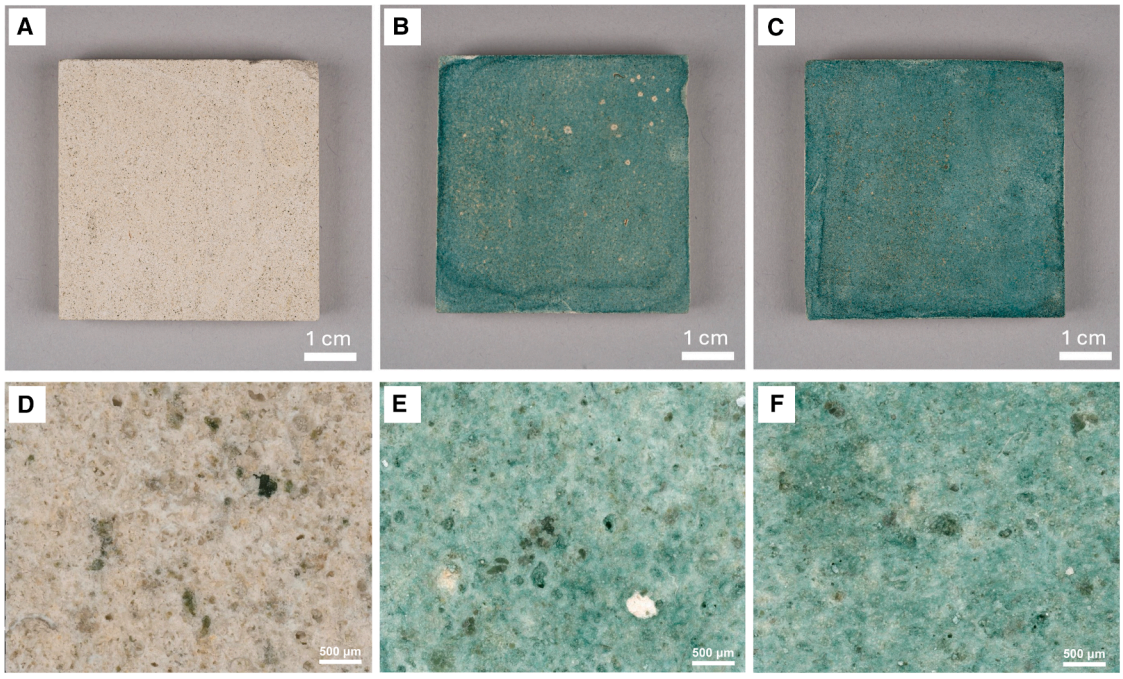

Figure 5. Surface documentation of uncolonized and biocolonized samples

Macroscopic documentation and microscopic images of uncolonized and biocolonized (dual-species and mono-species SABs) samples. Scale bar length in upper panels = 1 cm. Scale bar length in lower panels = 500 µm.

Table 2. Surface roughness assessment of uncolonized and biocolonized samples

	Uncolonized	Dual-species biofilm	Mono-species biofilm
Ra [μm][a]	11.2 ± 4.2	8.2 ± 4.1	8.9 ± 3.7
Rz [μm][b]	72.3 ± 27.2	52.0 ± 21.3	55.8 ± 22.1

Surface roughness expressed as Ra [μm] and Rz [μm], including standard deviations, of uncolonized and biocolonized (dual-species and mono-species SABs) samples.

[a]Arithmetical mean of all peak-valley heights of the assessed profile; 30 profiles for each sample were considered.

[b]Sum of the vertical distances of the five highest (peaks) and the five deepest (valleys) values of the assessed profile; 30 profiles of each sample were considered.

mean and dispersion of the respective distributions, represented in Figure 2.

Having established the comparability of the benchtop and portable instruments' application on a reference, non-absorbing, and uncolonized polymeric surface, the investigation was extended to uncolonized and biocolonized Lecce stone samples. These mineral substrates enabled assessing the applicability and robustness of the portable approach under conditions that more closely mimic common real-world scenarios.

Application of benchtop and portable measurement methods to laboratory biocolonized samples

Surface morphology and subaerial biofilms structure

Both laboratory-grown SABs homogeneously covered the specimens' surface both at the macro- and micro-scale, as documented by photographic (Figures 5A–5C) and microscopic documentation (Figures 5D–5F). The biofilms had a measurable impact on the surface roughness, i.e., a reduction of both Ra and Rz values (Table 2), as SABs (EPS and microorganisms) filled the superficial voids and stone discontinuities,[20,21] leading to an overall reduction of the surface macro-irregularities.

The cross-sections microscopic observation showed that the dual-species biofilm continuously covers the stone surface (Figure S2). The green biofilm was clearly detected on the top, with good adhesion to the substrate following the stone's superficial morphology. No clear sign of endolithic growth was observed. In this case, limited biofilm thickness was measured (around 10 μm). This could be due to possible mechanical effects during sample preparation (sampling, resin embedding, and polishing), leading to a reduction of the biofilm cross-section thickness. Alternative embedding methods are under consideration to reduce such an effect.

Observations of the surface morphology by SEM confirmed the consistent and complete biofilm coverage of the stone substrate (Figure 6), including a coating-like effect on the pore walls. The characteristic textural features of the Lecce stone, including macro-crystals and clustered finer ones, were no longer visible. In the colonized specimens, aggregates of microorganisms and EPS formed a continuous biological layer, conferring new morphological features to the surface compared to the uncolonized samples (Figures 6A–6C). The surface of the dual-species biofilm appeared more complex than the mono-species one (Figure 6B and 6C) due to the presence of more cellular clusters that contributed to the creation of peaks and valleys at the micro-scale on the surface. Individual cells of *Synechocystis* sp. with a rod shape can be easily recognized in both types of biofilms. They are attached to the surface embedded in the EPS (Figures 6E and 6F). In Figure 6E, the EPS has a filamentous shape, where cells are barely visible, a structure that was not observed in the mono-species biofilm. It can be assumed that this is connected with the presence of smaller *B. subtilis* cells and the production of different polymeric substances. It is worth noting that the vacuum conditions required for SEM observations may impact the biofilm structure by causing the

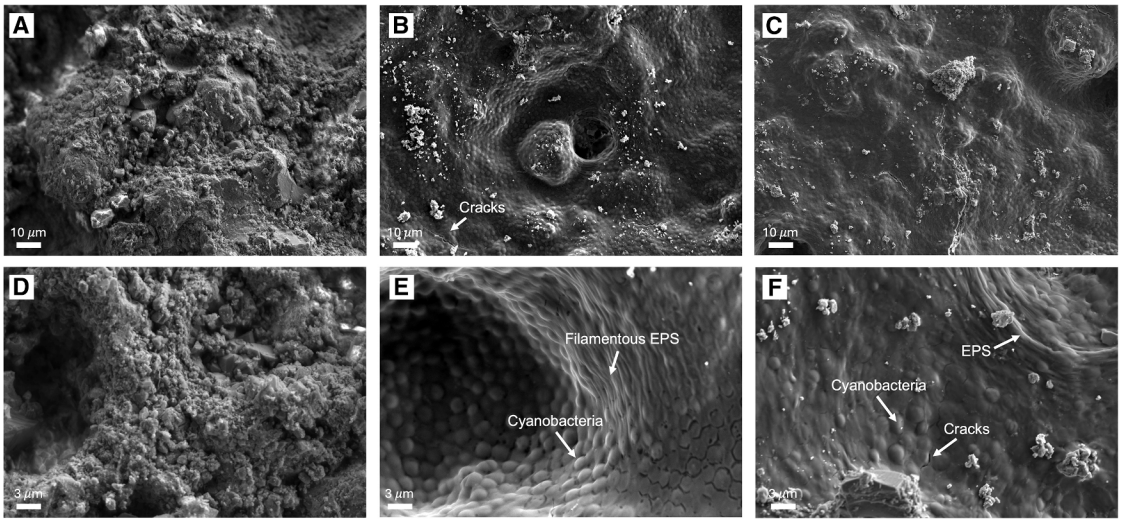

Figure 6. SEM observation of uncolonized and colonized stone surfaces

SEM images of the surface of (A and D) uncolonized Lecce stone sample, (B and E) dual-species biocolonized sample, and (C and F) mono-species biocolonized sample. Scale bar length in panels a, b, and c = 10 μm. Scale bar length in panels d, e, and f = 3 μm.

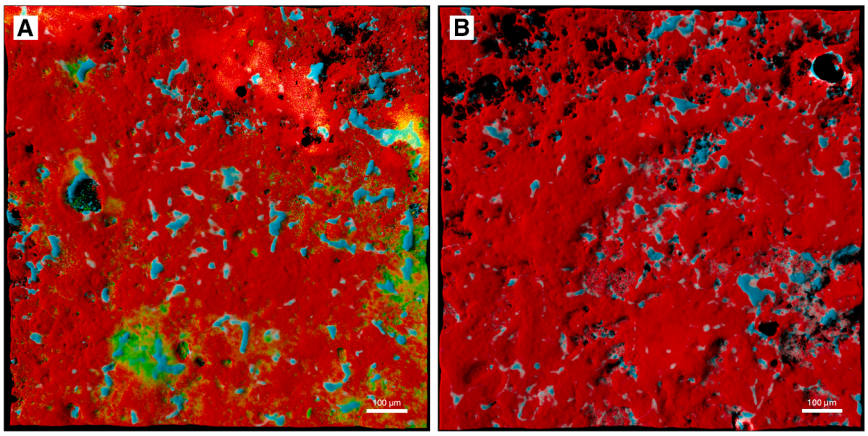

Figure 7. CLSM analysis of SABs on Lecce stone

Confocal laser scanning images of (A) dual-species and (B) mono-species biofilm growth on Lecce stone samples (photos) and the related properties (table). Color key: *Synechocystis* sp. PCC 6803 (phototroph), red (autofluorescence); *B. subtilis* NCIB 3610 (chemotroph) green, (Syto9); EPS (polysaccharide portion), light blue (ConA). Data in Table represent the means ± SD of independent measurements. According to the statistical analysis (t test, *p*-value <0.05), sharing the same letter means no statistically significant difference. Scale bar length in panels = 100 µm.

dehydration of both the EPS and the cells, ultimately leading to volume shrinkage and loss of tridimensional features.[22] In some cases, cracks in the biofilm were also observed. Consequently, SEM investigations of the biofilm were optimized to minimize exposure to high-vacuum conditions.

Confocal laser scanning images (CLSM) allowed the observation of the complex biofilm architecture. Compared to the SEM, CLSM observations provided a broader evaluation of the surface average conditions due to the larger scale of the investigated areas. The images in Figure 7 correspond to the tridimensional blend reconstruction obtained from the confocal image series with the dedicated IMARIS software.

The microscopic analysis shows the presence of EPS and a continuous biofilm covering the surface, indicative of a mature SAB in both mono- and dual-species systems.[20] Furthermore, some different features between the two biofilms were highlighted. The dual-species biofilm exhibited a more homogeneous coverage of the surface (Figure 7A), whereas the mono-species biofilm presented more gaps in its overall architecture. The differences in homogeneity were also confirmed by the values of the total biomass, which is higher for the dual-species than for the mono-species, with statistical significance (*p*-value = 0.022). The biomass measurements (Table 3) also confirmed the coexistence of both microorganisms in the dual-species biofilm, though not in identical proportions. As reported in the literature,[20–22] compositional shifts occur during development due to species-specific growth rates, metabolic interactions, and environmental conditions. Cross-feeding and spatial structuring are indeed intrinsic to multi-species biofilm systems.[23–27] The green portion in the dual-species biofilm revealed preferential locations of *B. subtilis* NCIB 3610 around the porosities and in the areas richer in EPS (blue signal, Con A). A slight difference is also reported in the biomass value related to the ConA signal (*p*-value = 0.036), higher for the dual-species. However, only the extracellular glycoconjugates were detected with this dye, and other differences may be found in other components of the EPS (i.e., lipids, proteins, eDNA). However, numerous studies have shown that cyanobacteria mainly produce EPS composed of polysaccharides.[14,28,29] Moreover, Villa et al. (2023)[14] demonstrated that carbohydrates were the predominant components of EPS in these lab-scale model systems compared to proteins and eDNA. CLSM also permits measuring the biofilm thickness. Images were captured as bottom-to-top slices from the substrate (stone) to the biofilm (from 0 to 0 fluorescent signal). Thus, a thickness of 28.0 ± 2.2 µm was calculated for the dual-species biofilm and 25.5 ± 3.5 µm for the mono-species. The CLSM results complement the cross-section observation by optical microscopy with precise and high resolution information about the SABs' thickness, also thanks to the fact that no sample manipulation is needed as opposed to the latter method. This clearly reduces any potential unwanted alteration induced by the sample preparation operations. Nonetheless, cross-section observation provides critical information regarding the SABs' thickness homogeneity of adhesion to the substrate, and the type of growth (i.e., epilithic or endolithic) of the biofilm, hardly detectable with the CLSM.

Table 3. Biomass analysis of SABs on Lecce stone

	Biomass ($\mu m^3/\mu m^2$)			
	Autofluo (*Synechocystis* sp. PCC6803)	SYTO9 (*B. subtilis* NCIB 3610)	ConA (EPS)	Total (Autofluo + ConA)
Dual-species	4.48 ± 0.36[a]	1.97 ± 0.15	3.32 ± 0.36[a]	7.80 ± 0.65[a]
Mono-species	3.92 ± 0.37[a]	/	2.73 ± 0.25[b]	6.65 ± 0.37[b]

Properties related to confocal laser scanning images of mono- and dual-species biofilms. Data in Table represent the means ± SD of independent measurements. According to the statistical analysis (t test, *p*-value <0.05), sharing the same letter means no statistically significant difference.

Drop absorption time and water contact angle on mono- and dual-species

Both benchtop and portable measurement methods were applied to biocolonized and uncolonized laboratory Lecce stone samples.

Drop absorption time results showed no significant difference when measured by the two methods for uncolonized and mono-species biofilm samples (Figure 8; Table 4). There is, instead, a very limited difference between the two methods for the

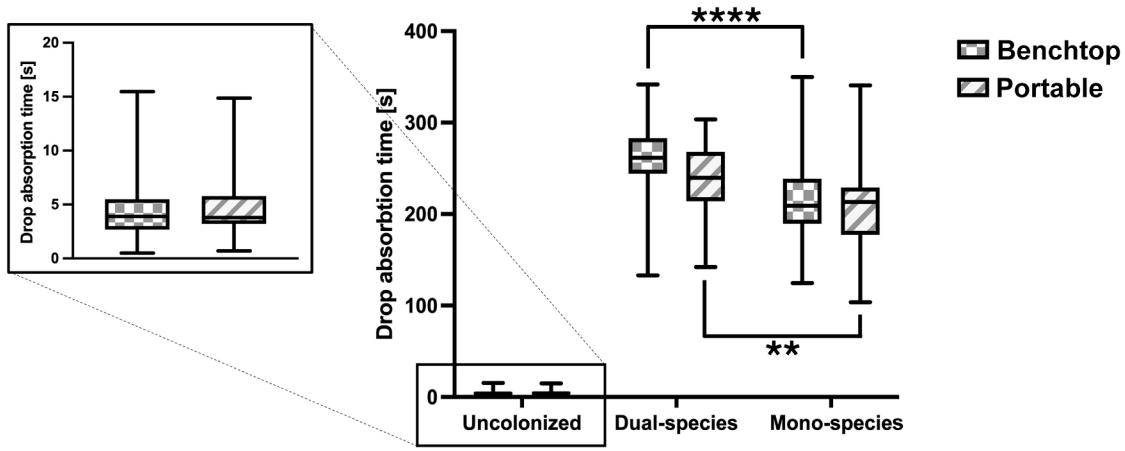

Figure 8. Drop absorption time on uncolonized and biocolonized samples

Drop absorption time [s] obtained on uncolonized and biocolonized (dual-species and mono-species SABs) Lecce stone samples, measured with the benchtop and the portable measurement methods, respectively. Keys: * for p-value $\leq$ 0.05; ** for p-value $\leq$ 0.01; *** for p-value $\leq$ 0.001; **** for p-value $\leq$ 0.0001. Error bars indicate standard deviation.

dual-species biocolonized samples (Figure 8; Table 4). Data dispersion is significant for both approaches and may be attributed to the high inherent chemical and morphological heterogeneity of this type of substrate compared to the non-absorbing polymeric reference. As observed in surface morphology and subaerial biofilms structure, SABs' thickness and architecture may differ in different areas of the sample, leading to local variability in the drop absorption times. In addition, the inherent stone porosity and chemical and physical heterogeneity can also influence drop absorption time results, as indicated by the data dispersion that was also observed in the uncolonized samples.

Significant differences, instead, emerged from the comparison between the WCA values measured according to the two methods: in particular, values measured with the portable instrument are around 25% higher than those obtained by the benchtop approach (Figure 9; Table 5). A possible explanation could be linked to the different dosing methods previously commented on. In the case of the benchtop instrument, the drop comes in contact with the surface while still being attached to the dosing syringe. Therefore, some initial water absorption may occur before the drop reaches stability conditions (i.e., the drop is fully released by the syringe and stable enough for correct focusing), which are required before the measurement can start.[30] In the case of the portable instrument, the drop is sprayed onto the surface at a constant pressure (Video S1) without direct contact between the dosing unit and the investigated surface, allowing for a more precise discrimination between the end of the dosing and the beginning of the absorption. Given that no significant variation in drop volume was observed in the preliminary tests on the reference slab (Section "drop volume and water contact angle results"), the effect of the different dosing system greatly affects WCA values. As an instantaneous measurement, WCA is highly sensitive to initial droplet dynamics, which are influenced by the dosing system. Conversely, drop absorption time is measured over a longer duration and, with the same delivered volume, is less affected by differences in droplet deposition as well as by potential surface heterogeneities or local microbial activity.

WCA and drop absorption time also allowed to identify differences among dual- and mono-species biofilm. Despite some discrepancies between the two methods (benchtop and portable) in terms of measured WCA (while showing very good agreement in drop absorption time), the observed trends are entirely consistent. Thus, the same conclusions can be drawn regardless of the method used, even though the absolute WCA values differ between the two approaches (Figures 8 and 9). In the case of the mono-species biofilm, the drop absorption time increased from about 5 s to about 3.5 min. For the dual-species biofilm, the absorption time further increased, reaching about 4 min. This represents an increase of about 14% compared to the mono-species biofilm (p-value $\leq$ 0.01) (Figure 8), highlighting its stronger impact on surface wettability. This effect is probably related to the larger production of EPS and the more compact biological structure of the dual-species biofilm, as shown in surface morphology and subaerial biofilms structure. EPS is a critical factor that significantly contributes to decreasing wettability.[17,31,32] Statistically significant differences were also reported in the WCA values (p-value $\leq$ 0.01) (Figure 9). In any case, results indicated that the presence of both mono- and dual-species biofilms is associated with prolonged absorption time compared to non-colonized conditions.

Table 4. Drop absorption times and standard deviations on uncolonized and biocolonized samples

Drop absorption time [s]		
Instrument	Benchtop	Portable
Uncolonized	4.60 ± 2.89	5.49 ± 3.69
Dual-species	258.96 ± 40.60	238.29 ± 34.70
Mono-species	218.58 ± 49.84	208.25 ± 47.82

Drop absorption time [s] obtained on uncolonized and biocolonized (dual-species and mono-species SABs) Lecce stone samples, measured with the benchtop and the portable measurement methods, respectively.

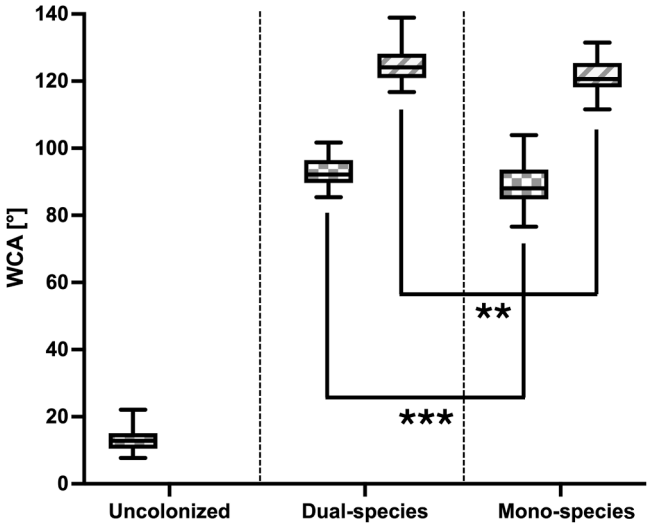

Figure 9. WCA on uncolonized and biocolonized samples

Water contact angle [°] values obtained on uncolonized and biocolonized (dual-species and mono-species SABs) Lecce stone samples, respectively with the benchtop and the portable measurement methods. Legenda: * for p-value $\leq$ 0.05; ** for p-value $\leq$ 0.01; *** for p-value $\leq$ 0.001; **** for p-value $\leq$ 0.0001. Error bars indicate standard deviation.

The dual-species biofilm is also characterized by a higher WCA if compared to the mono-species. This may be explained by the more complex nano- and micro-structured surface in the case of phototroph-chemotroph interactions.[20] WCA values measured with the benchtop instrument were around 90° while the WCA values obtained with the portable approach were greater than 120° (Figure 9; Table 5), indicating hydrophobic conditions immediately after drop stabilization. This is even more significant considering the hydrophobic threshold of 65° that some authors[12] suggest as a reference threshold,[12] particularly for biomaterials,[6] as previously mentioned. Furthermore, after 30 s, which is the time specified by the standard,[8] the values remained above 65°. These data clearly demonstrate that biofilms confer water-repellent properties to the Lecce stone surface at least for the first 30 s.

Both the prolonged drop absorption time and the high first WCA values describe a biofilm that provides water-repellency to the surface, according to the categories defined by Leelamanie et al. (2008).[19] Such results are in agreement with the literature[14,16–18] and highlight that the presence of SABs on built surfaces can potentially provide beneficial effects against water-related weathering mechanisms.

It has to be underlined that the actual role of SABs is still difficult to define due to the complexity of the SAB-substrate-atmosphere ecosystem.[15,33–36] Laboratory biocolonized samples have indeed shown a reduced capillary water absorption rate compared to uncolonized samples.[14,16,18,37] Furthermore, it is reasonable to assume that they may delay capillary water absorption and water evaporation.[18] SABs may indeed be able to maintain more constant moisture conditions, and therefore reduce hygric stresses, slowing down the rate of moisture exchange between the substrates and the environment.[15] However, the experimental evaluation of such effects is still very challenging due to the difficulty of growing uniform and resilient biofilms in laboratory conditions and their inherent variability.

It is also worth noting the potential influence of environmental conditions on the measured values. The laboratory experiments were conducted under controlled and constant temperature and relative humidity conditions. Such a level of control cannot be ensured when measurements are conducted on-site, particularly outdoors, where natural climatic fluctuations are often unavoidable. It is therefore important to report critical environmental data during the measurement, along with any relevant microclimatic conditions occurring in the preceding days that may impact the results (e.g., rain events, heat waves) to ensure meaningful interpretation of the data.

Table 5. WCA values and standard deviations on uncolonized and biocolonized samples

WCA [°]		
Instrument	Benchtop	Portable
Uncolonized	13.56 ± 3.94	/
Dual-species	92.91 ± 4.07	124.02 ± 5.56
Mono-species	88.97 ± 6.16	120.50 ± 5.44

WCA [°] obtained on uncolonized and biocolonized (dual-species and mono-species SABs) Lecce stone samples, measured with the benchtop and the portable measurement methods, respectively.

Relationship between portable and benchtop measurement methods

Benchtop and portable datasets of drop absorption times and WCA results were related, each set being acquired on the same biocolonized surfaces. Each set consisted of 15 measurements. Based on these, the mean and standard error were computed. Then, a regression analysis was carried out to relate the two measurements. The results are shown in Figure 10.

For WCA, the two methods provide different results. The mean WCA fit yields a slope of 0.788 ± 0.524, i.e., with a large uncertainty. The R^2 = 0.334 shows that only a small portion of the variability can be accounted for. Thus, the portable measurements cannot be related straightforwardly to those obtained with the benchtop instrument. On the contrary, the mean drop absorption time fit yields a slope of 1.237 ± 0.105, with a small relative uncertainty. The R^2 = 0.967 demonstrates that most of the variability is captured by the linear model. Thus, in the case of drop absorption time, the portable measurements can be mapped using a multiplicative conversion factor to the benchtop instrument results with a small comparative error. In any case, it must be emphasized that, in terms of drop absorption time, the differences between the two methods were minimal.

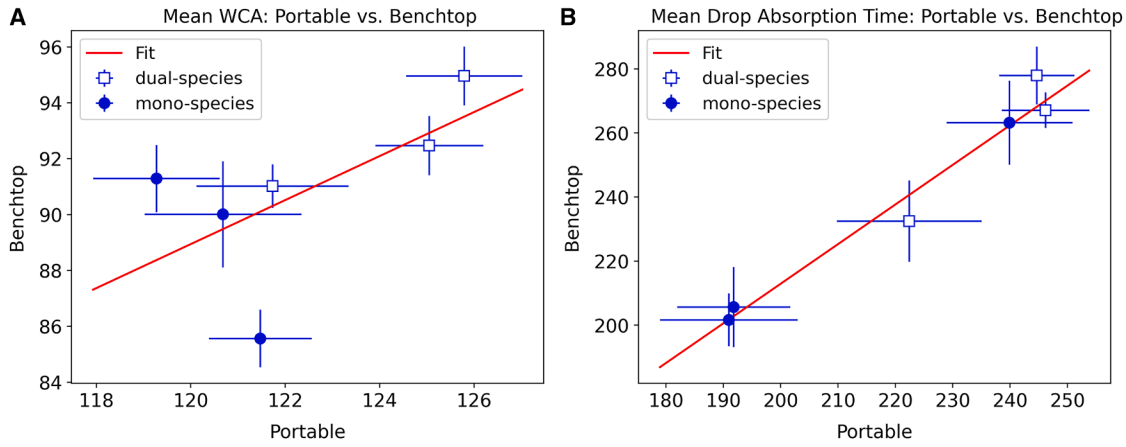

Figure 10. Correlation between benchtop and portable method

Results of the regression analysis to relate the two methods for (A) WCA and (B) drop absorption time. Error bars indicate standard error.

Conclusions

In this study, the application of a portable approach for on-site WCA measurements was validated against a conventional benchtop method for the first time. The robustness and consistency of the WCA results obtained with the two methods during the preliminary evaluation on a reference, non-absorbing surface confirm the strong potential of the portable approach as an alternative to standard, lab-based measurements of substrates with such characteristics.

The comparative assessment of biocolonized porous substrates provided more challenging testing conditions, although closer to real-world scenarios. In this case, significant differences between the two methods were observed for the WCA values, but the observed trends (i.e., variations in the WCA values due to different surface conditions according to the same test method) remained remarkably consistent within the same method, thus confirming the reliability of the portable approach against the standard one. Such differences are likely linked to the different geometry and working conditions of the two instruments, particularly the water dosing system. Therefore, further investigation is needed to unveil the consistently higher WCA values obtained with the portable method, support the interpretation of absolute WCA values in complex conditions, and refine the interpretation of WCA measurements obtained through both approaches.

On the other hand, the measurement of drop absorption time showed only minimal differences between the two methods, confirming the reliability of the portable one for the on-site assessment of drop absorption times on differently oriented surfaces. After proper calibration with laboratory results, this parameter could further expand the applicability of the portable method to investigate a broader set of questions, such as the comparative evaluation of different surface weathering conditions, the impact of biofilm on water-related properties,

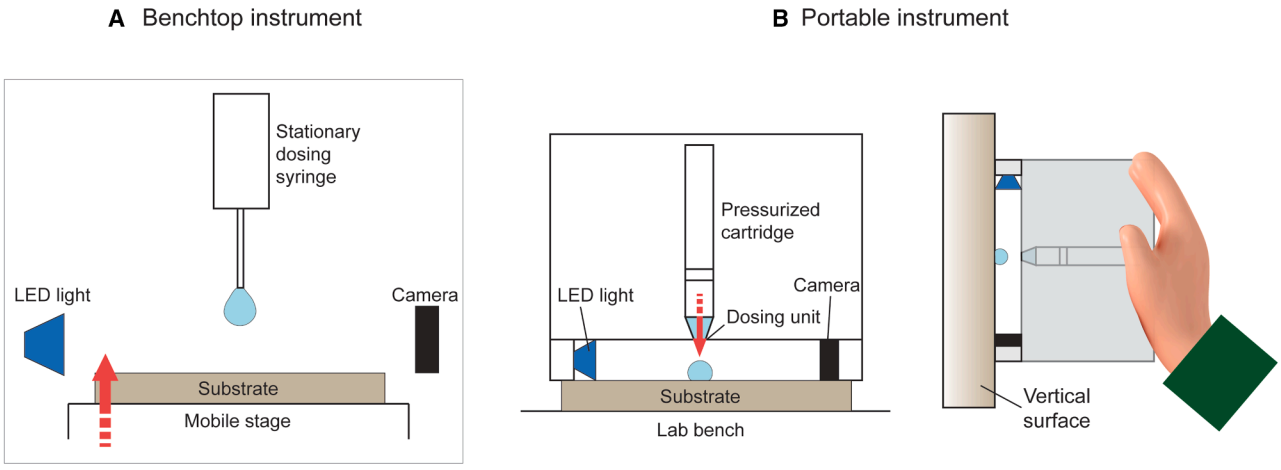

Figure 11. Experimental set-up of benchtop and portable measurements

Graphic representation of the experimental setup of (A) benchtop instrument and (B) portable instrument, in horizontal and vertical orientations. Proportions between instruments do not represent the real conditions.

and the performance and durability of surface conservation treatments.

Furthermore, the results highlighted differences between mono-species and dual-species biofilm, with the dual-species providing the highest increase in terms of both WCA and drop absorption time. Therefore, this study also confirms the potential applicability of WCA measurements to characterize different SAB-substrate systems and their impact on architectural surfaces.

Ultimately, this study provides the first contribution to establishing a methodology for investigating SABs-induced alterations of water absorption properties on site in a less invasive (i.e., reduced amount of water needed, reduced contact areas) and potentially more precise way compared to other conventionally employed methods.

Limitations of the study

The comparative evaluation of benchtop and portable approaches was initially validated on a reference, non-absorbing polymeric surface and then extended to stone specimens, with and without subaerial biofilm colonization. A single reference stone material, widely characterized in the literature, was used. Therefore, further investigations are necessary to assess how different and more complex combinations of compositional and physical properties of mineral substrates affect water-related behavior in the presence of SABs, as measured by WCA. Additionally, all experiments were conducted in the laboratory, so the study is limited to WCA and drop absorption times measured under controlled and stable temperature and relative humidity conditions. Future work should also expand the experimental framework to include a broader range of biofilms and microbial communities, which may exhibit different structural and chemical characteristics, potentially influencing surface wettability in various ways. Finally, the discrepancies observed in WCA values between benchtop and portable instruments on porous substrates highlight the need for further investigation into the effects of drop deposition methods and surface interactions, in order to improve the interpretation and comparability of results obtained with different measurement setups.

RESOURCE AVAILABILITY

Lead contact

Further information and requests for resources and reagents should be directed to and will be fulfilled by the lead contact, Davide Gulotta (dgulotta@getty.edu).

Materials availability

This study did not generate new unique reagents.

Data and code availability

- Any additional information required to reanalyze the data reported in this article is available from the lead contact upon request.
- This article does not report original code.

AUTHOR CONTRIBUTIONS

Conceptualization, LB, DG, and SG; methodology, LB, DG, SG, FC, FV, and GG; investigation, LB, DG, FV, and GG; writing—original draft, LB and GG; writing—review and editing, LB, DG, SG, FC, FV, and LT; funding acquisition, DG and LT; resources, DG and LT; supervision, DG, SG, and FC.

DECLARATION OF INTERESTS

The authors declare no competing interests.

STAR★METHODS

Detailed methods are provided in the online version of this paper and include the following:

- KEY RESOURCES TABLE
- EXPERIMENTAL MODEL AND SUBJECT DETAILS
- METHOD DETAILS
  - Monitoring testing conditions
  - Test on reference material
  - Benchtop instrument measurements
  - Portable instrument measurements
- TEST ON BIOCOLONIZED SAMPLES
  - Samples preparation
  - SAB architecture and characterization
  - Benchtop contact angle measurements
  - Portable contact angle measurements
- QUANTIFICATION AND STATISTICAL ANALYSIS
  - Statistical variability analysis and sample size determination
  - Correlation between benchtop and portable measurement methods

SUPPLEMENTAL INFORMATION

Supplemental information can be found online at https://doi.org/10.1016/j.isci.2025.113282.

Received: March 28, 2025
Revised: June 9, 2025
Accepted: July 30, 2025
Published: August 5, 2025

REFERENCES

1. Prîkryl, R., and Smith, B.J. (2007). In Building Stone Decay: From Diagnosis to Conservation, *271*, R. Prîkryl and B.J. Smith, eds. (Special Publication).
2. Siegesmund, S., Weiss, T., and Vollbrecht, A. (2002). Natural stone, weathering phenomena, conservation strategies and case studies: introduction. Geol. Soc. Spec. Publ. *205*, 1–7. https://doi.org/10.1144/GSL.SP.2002.205.01.01.
3. Gorbushina, A.A., and Broughton, W.J. (2009). Microbiology of the atmosphere-rock interface: How biological interactions and physical stresses modulate a sophisticated microbial ecosystem. Annu. Rev. Microbiol. *63*, 431–450. https://doi.org/10.1146/annurev.micro.091208.073349.
4. Gulotta, D., and Toniolo, L. (2022). Preliminary Investigations, Condition Assessment, and Mapping of the Deterioration Patterns. In Conserving Stone Heritage, F. Gherardi and P.N. Maravelaki, eds. (Springer), pp. 1–36. https://doi.org/10.1007/978-3-030-82942-1_1.
5. Kung, C.H., Sow, P.K., Zahiri, B., and Mérida, W. (2019). Assessment and Interpretation of Surface Wettability Based on Sessile Droplet Contact Angle Measurement: Challenges and Opportunities. Adv. Mater. Interfaces *6*, 1900839. https://doi.org/10.1002/admi.201900839.
6. Nguyen-Tri, P., Tran, H.N., Plamondon, C.O., Tuduri, L., Vo, D.V.N., Nanda, S., Mishra, A., Chao, H.P., and Bajpai, A.K. (2019). Recent progress in the preparation, properties and applications of superhydrophobic nano-based coatings and surfaces: A review. Prog. Org. Coating *132*, 235–256. https://doi.org/10.1016/j.porgcoat.2019.03.042.
7. Della Volpe, C., Penati, A., Peruzzi, R., Siboni, S., Toniolo, L., and Colombo, C. (2000). Combined effect of roughness and heterogeneity on contact angles: the case of polymer coating for stone protection. J. Adhes. Sci. Technol. *14*, 273–299. https://doi.org/10.1163/156856100742555.

8. EN 15802 Conservation of cultural property - Test methods - Determination of static contact angle. (2009).
9. Young, T. (1805). III. An essay on the cohesion of fluids. Philos. Trans. R. Soc. Lond. *95*, 65–87. https://doi.org/10.1098/rstl.1805.0005.
10. Marmur, A., Della Volpe, C., Siboni, S., Amirfazli, A., and Drelich, J.W. (2017). Contact angles and wettability: Towards common and accurate terminology. Surf. Innovations *5*, 3–8. https://doi.org/10.1680/jsuin.17.00002.
11. Jeevahan, J., Chandrasekaran, M., Britto Joseph, G., Durairaj, R.B., and Mageshwaran, G. (2018). Superhydrophobic surfaces: a review on fundamentals, applications, and challenges. J. Coat. Technol. Res. *15*, 231–250. https://doi.org/10.1007/s11998-017-0011-x.
12. Vogler, E.A. (1998). Structure and reactivity of water at biomaterial surfaces. Adv. Colloid Interface Sci. *74*, 69–117.
13. Berti, L., Arfelli, F., Villa, F., Cappitelli, F., Gulotta, D., Ciacci, L., Bernardi, E., Vassura, I., Passarini, F., Napoli, S., and Goidanich, S. (2024). LCA as a Complementary Tool for the Evaluation of Biocolonization Management: The Case of Palazzo Rocca Costaguta. Heritage *7*, 6871–6890. https://doi.org/10.3390/heritage7120318.
14. Villa, F., Ludwig, N., Mazzini, S., Scaglioni, L., Fuchs, A.L., Tripet, B., Copié, V., Stewart, P.S., and Cappitelli, F. (2023). A desiccated dual-species subaerial biofilm reprograms its metabolism and affects water dynamics in limestone. Sci. Total Environ. *868*, 161666. https://doi.org/10.1016/j.scitotenv.2023.161666.
15. Berti, L., Villa, F., Toniolo, L., Cappitelli, F., and Goidanich, S. (2024). Methodological challenges for the investigation of the dual role of biofilms on outdoor heritage. Sci. Total Environ. *954*, 176450. https://doi.org/10.1016/j.scitotenv.2024.176450.
16. Berti, L., Villa, F., Cappitelli, F., Napoli, S., Barbieri, A., Toniolo, L., Gulotta, D., and Goidanich, S. (2023). Contact angle as a non-destructive method to determine wettability changes induced by sub-aerial biofilms on built heritage porous substrates. In Proceedings of Art'23: 14th International Conference on Non-Destructive Investigations and Microanalysis for the Diagnostics and Conservation of Cultural and Environmental Heritage, *15*, pp. 147–152. https://www.ndt.net/search/docs.php3?id=28922.
17. Sanmartín, P., Villa, F., Cappitelli, F., Balboa, S., and Carballeira, R. (2020). Characterization of a biofilm and the pattern outlined by its growth on a granite-built cloister in the Monastery of San Martiño Pinario (Santiago de Compostela, NW Spain). Int. Biodeterior. Biodegrad. *147*, 104871. https://doi.org/10.1016/j.ibiod.2019.104871.
18. Schröer, L., De Kock, T., Godts, S., Boon, N., and Cnudde, V. (2022). The effects of cyanobacterial biofilms on water transport and retention of natural building stones. Earth Surf. Process. Landf. *47*, 1921–1936. https://doi.org/10.1002/esp.5355.
19. Leelamanie, D.A.L., Karube, J., and Yoshida, A. (2008). Characterizing water repellency indices: Contact angle and water drop penetration time of hydrophobized sand. Soil Sci. Plant Nutr. *54*, 179–187. https://doi.org/10.1111/j.1747-0765.2007.00232.x.
20. Villa, F., Pitts, B., Lauchnor, E., Cappitelli, F., and Stewart, P.S. (2015). Development of a laboratory model of a phototroph-heterotroph mixed-species biofilm at the stone/air interface. Front. Microbiol. *6*, 1251. https://doi.org/10.3389/fmicb.2015.01251.
21. Mony, C., Vandenkoornhuyse, P., Bohannan, B.J.M., Peay, K., and Leibold, M.A. (2020). A landscape of opportunities for microbial ecology research. Front. Microbiol. *11*, 561427. https://doi.org/10.3389/fmicb.2020.561427.
22. Ramírez, M., Hernández-Mariné, M., Novelo, E., and Roldán, M. (2010). Cyanobacteria-containing biofilms from a Mayan monument in Palenque, Mexico. Biofouling *26*, 399–409.
23. Hayashi, S., Itoh, K., and Suyama, K. (2011). Growth of the cyanobacterium synechococcus leopoliensis CCAP1405/1 on agar media in the presence of heterotrophic bacteria. Microbes Environ. *26*, 120–127. https://doi.org/10.1264/jsme2.ME10193.
24. Beliaev, A.S., Romine, M.F., Serres, M., Bernstein, H.C., Linggi, B.E., Markillie, L.M., Isern, N.G., Chrisler, W.B., Kucek, L.A., Hill, E.A., et al. (2014). Inference of interactions in cyanobacterial-heterotrophic co-cultures via transcriptome sequencing. ISME J. *8*, 2243–2255. https://doi.org/10.1038/ismej.2014.69.
25. Cole, J.K., Hutchison, J.R., Renslow, R.S., Kim, Y.M., Chrisler, W.B., Engelmann, H.E., Dohnalkova, A.C., Hu, D., Metz, T.O., Fredrickson, J.K., and Lindemann, S.R. (2014). Phototrophic biofilm assembly in microbial-mat-derived unicyanobacterial consortia: Model systems for the study of autotroph-heterotroph interactions. Front. Microbiol. *5*, 109. https://doi.org/10.3389/fmicb.2014.00109.
26. Valverde, A., Makhalanyane, T.P., Seely, M., and Cowan, D.A. (2015). Cyanobacteria drive community composition and functionality in rock-soil interface communities. Mol. Ecol. *24*, 812–821. https://doi.org/10.1111/mec.13068.
27. Ma, J., Guo, T., Ren, M., Chen, L., Song, X., and Zhang, W. (2022). Cross-feeding between cyanobacterium Synechococcus and Escherichia coli in an artificial autotrophic–heterotrophic coculture system revealed by integrated omics analysis. Biotechnol. Biofuels Bioprod. *15*, 69. https://doi.org/10.1186/s13068-022-02163-5.
28. Pereira, S., Micheletti, E., Zille, A., Santos, A., Moradas-Ferreira, P., Tamagnini, P., and De Philippis, R. (2011). Using extracellular polymeric substances (EPS)-producing cyanobacteria for the bioremediation of heavy metals: Do cations compete for the EPS functional groups and also accumulate inside the cell? Microbiology *157*, 451–458. https://doi.org/10.1099/mic.0.041038-0.
29. Rossi, F., and De Philippis, R. (2015). Role of cyanobacterial exopolysaccharides in phototrophic biofilms and in complex microbial mats. Life *5*, 1218–1238. https://doi.org/10.3390/life5021218.
30. Yilbas, B.S., Al-Sharafi, A., Ali, H., and Al-Aqeeli, N. (2017). Dynamics of a water droplet on a hydrophobic inclined surface: Influence of droplet size and surface inclination angle on droplet rolling. RSC Adv. *7*, 48806–48818. https://doi.org/10.1039/c7ra09345d.
31. Czaczyk, K., and Myszka, K. (2007). Biosynthesis of extracellular polymeric substances (EPS) and its role in microbial biofilm formation. Pol. J. Environ. Stud. *16*, 799–806.
32. Flemming, H.C. (2016). EPS - then and now. Microorganisms *4*, 41. https://doi.org/10.3390/microorganisms4040041.
33. Villa, F., Stewart, P.S., Klapper, I., Jacob, J.M., and Cappitelli, F. (2016). Subaerial Biofilms on Outdoor Stone Monuments: Changing the Perspective Toward an Ecological Framework. Bioscience *66*, 285–294. https://doi.org/10.2307/90007580.
34. Favero-Longo, S.E., and Viles, H.A. (2020). A review of the nature, role and control of lithobionts on stone cultural heritage: weighing-up and managing biodeterioration and bioprotection. World J. Microbiol. Biotechnol. *36*, 100. https://doi.org/10.1007/s11274-020-02878-3.
35. Pinna, D. (2014). Biofilms and lichens on stone monuments: Do they damage or protect? Front. Microbiol. *5*, 133. https://doi.org/10.3389/fmicb.2014.00133.
36. Liu, X., Qian, Y., Wu, F., Wang, Y., Wang, W., and Gu, J.-D. (2022). Biofilms on stone monuments: biodeterioration or bioprotection? Trends Microbiol. *30*, 816–819. https://doi.org/10.1016/j.tim.2022.05.012.
37. Concha-Lozano, N., Gaudon, P., Pages, J., de Billerbeck, G., Lafon, D., and Eterradossi, O. (2012). Protective effect of endolithic fungal hyphae on oolitic limestone buildings. J. Cult. Herit. *13*, 120–127. https://doi.org/10.1016/j.culher.2011.07.006.
38. Mills, L.A., McCormick, A.J., and Lea-Smith, D.J. (2020). Current knowledge and recent advances in understanding metabolism of the model cyanobacterium Synechocystis sp. PCC 6803 Bioscience Reports. Biosci. Rep. *40*, BSR20193325. https://doi.org/10.1042/BSR20193325.
39. Arnaouteli, S., Bamford, N.C., Stanley-Wall, N.R., and Kovács, Á.T. (2021). *Bacillus subtilis* biofilm formation and social interactions. Nat. Rev. Microbiol. *19*, 600–614. https://doi.org/10.1038/s41579-021-00540-9.

40. Bugani, S., Camaiti, M., Morselli, L., Van De Casteele, E., and Janssens, K. (2007). Investigation on porosity changes of Lecce stone due to conservation treatments by means of x-ray nano- And improved micro-computed tomography: Preliminary results. X Ray Spectrom. *36*, 316–320. https://doi.org/10.1002/xrs.976.

41. Lubelli, B., Aguilar, A.M., Beck, K., De Kock, T., Desarnaud, J., Franzoni, E., Gulotta, D., Ioannou, I., Kamat, A., Menendez, B., et al. (2022). A new accelerated salt weathering test by RILEM TC 271-ASC: preliminary round robin validation. Mater. Struct. *55*, 238. https://doi.org/10.1617/s11527-022-02067-8.

42. Borgia, G.C., Camaiti, M., Cerri, F., Fantazzini, P., and Piacenti, F. (2000). Study of water penetration in rock materials by Nuclear Magnetic Resonance Tomography: hydrophobic treatment effects. J. Cult. Herit. *1*, 127–132.

43. Andriani, G.F. (2024). Petrophysical and Mechanical Properties of the Piromafo Stone Used in the Built Heritage of Apulia (SE Italy): A Comprehensive Laboratory Study. Geosciences *14*, 201. https://doi.org/10.3390/geosciences14080201.

44. Sanmartín, P., Villa, F., Silva, B., Cappitelli, F., and Prieto, B. (2011). Color measurements as a reliable method for estimating chlorophyll degradation to phaeopigments. Biodegradation *22*, 763–771. https://doi.org/10.1007/s10532-010-9402-8.

45. Nurkasanah, S., and Widodo, N. (2015). The effect of Different Media Content on Protease Activity *Bacillus subtilis*. Biotropika *3*, 104–106.

46. ISO 21920-2 - Geometrical Product Specifications (GPS) - Surface Texture: Profile (2021).

47. Wilhelm, K., Viles, H., and Burke, Ó. (2016). Low impact surface hardness testing (Equotip) on porous surfaces – advances in methodology with implications for rock weathering and stone deterioration research. Earth Surf. Process. Landf. *41*, 1027–1038. https://doi.org/10.1002/esp.3882.

STAR★METHODS

KEY RESOURCES TABLE

REAGENT or RESOURCE	SOURCE	IDENTIFIER
Bacterial and virus strains		
Synechocystis sp. PCC 6803	American Type Colture Collection (ATCC)	27184
Bacillus subtilis NCIB 3610	American Type Colture Collection (ATCC)	6051
Chemicals, peptides, and recombinant proteins		
SYTO9	ThermoFisher Scientific, Waltham, Massachusetts, USA	S34854
Concanavaline A Texas Red	ThermoFisher Scientific, Waltham, Massachusetts, USA	C825
BG11 medium	American Type Colture Collection (ATCC)	ATCC Medium 2661
TSB medium	Condalab, Madrid, Spain	1124
Technovit 2000 LC Fixierpaste	Kulzer GmbH, Hanau, Germany	
Software and algorithms		
JMP Pro 17.0.0	https://jmp.com	
RStudio	https://posit.com/	
Python libraries scipy and sklearn	https://pypi.org	
ImageJ	https://imagej.net/	
Imaris	Bitplane Scientific Software, Switzerland	
Kruss Advance Software v. 1.16.0.10201	A. KRÜSS Optronic, Hamburg, Germany	

EXPERIMENTAL MODEL AND SUBJECT DETAILS

Two types of SABs, a mono-species and a dual-species, were employed. The mono-species was composed of the phototroph *Synechocystis* sp. PCC 6803, while the dual-species of the same cyanobacterium and the chemotroph *Bacillus subtilis* NCIB 3610. *Synechocystis* sp. PCC 6803 is one of the most genetically and physiologically characterized cyanobacteria, frequently used in laboratory studies due to its ease of cultivation and well-understood metabolic pathways.[38] Likewise, *B. subtilis* is a widely studied chemotroph with well-established biofilm-forming capabilities.[39] Both microorganisms have been retrieved from stone monuments and ensure fast-growing SABs, making them ideal candidates for studies on microbial colonization and biofilm impacts on stone surfaces. These laboratory-grown SABs capture the essential features of biofilms inhabiting lithic substrates, including microcolonies of aggregated microorganisms, network-like structures, phototroph-chemoorganotroph interactions, resilience in harsh environments, and tolerance to biocides.[20] The choice of these model systems is justified by their reliability, reproducibility, ecological relevance, and compatibility with natural stone substrates.

METHOD DETAILS

Monitoring testing conditions

All tests were performed under controlled laboratory conditions. Temperature (T) and relative humidity (RH) were monitored with a HOBO Temperature/Relative Humidity data logger (LI-COR, Lincoln, Nebraska, USA) throughout the experiments to ensure consistent operational conditions. The average T and RH values, along with the respective standard deviations, are reported at the end of each paragraph of interest. The determination of the static contact angle was performed according to the EN 15802: 20098,[8] after adaptation for non-ideal surfaces as described in the following sections.

Test on reference material

Static water contact angle measurements were conducted on a reference non-absorbing polymeric surface (CP53 Reference Plate, A. KRÜSS Optronic, Hamburg, Germany) to compare the results obtained by the onsite portable and the laboratory benchtop instruments. The instrument manufacturer recommends this substrate as a reference for calibrating the droplet dosing volume. Its smooth and chemically homogeneous nature ensures reproducible dosing conditions (drop shape and volume) and accurate contact angle analysis. During the tests, temperature and relative humidity values were 20.8°C ± 0.2 and 45.4% ± 0.8, respectively.

Benchtop instrument measurements

The Kruss Drop Shape Analyzer (A.KRÜSS Optronic, Hamburg, Germany) was the laboratory benchtop instrument used for WCA measurements. The instrument is composed of a dosing syringe, a movable stage for the sample, an LED light source, and a camera with manual focus and zoom (Figure 11A). The system is software-controlled (Kruss Advance, A. KRÜSS Optronic, Hamburg, Germany). The reference slab was positioned on the stage, and a 5 μL drop was dispensed by the tip of the syringe needle. Then, the stage was moved until contact with the surface, and the drop was released by moving the syringe back to the initial position. For each measurement, a 10-s video at 60 frames per second (fps) was recorded, and data elaboration was performed a posteriori using the same software. After the drop stabilization on the surface (resulting in a stable and fully focused drop shape), the volume of the drop and the static water contact angle were calculated using the Young-Laplace model. The measurement was randomly repeated over the entire surface 50 times.

Portable instrument measurements

The portable Kruss Mobile Surface Analyzer instrument (A. KRÜSS Optronic, Hamburg, Germany) was used in laboratory conditions to measure WCAs and drop volumes on a reference slab for method validation. This instrument is a portable system composed of two dosing units connected to pressurized cartridges, an LED light source, and a camera with fixed focus and focal length (Figure 11B). The system is software-controlled (Advance, A. KRÜSS Optronic, Hamburg, Germany). The instrument was positioned on the reference slab, and two 5 μL water drops were dispensed with a 2-s time gap by the dosing units onto the surface. A 10-s video was recorded at 10 fps and elaborated a posteriori. After drop stabilization onto the surface (resulting in a stable and fully focused drop shape), the volume of each drop and the static water contact angle were calculated using the Young-Laplace model. The measurement was repeated over the entire surface 25 times (50 drops in total). The instrument geometry and the type of drop delivery (pressure drop ejection) allow for working on-site on non-horizontal surfaces (Figure 11B). With this device, therefore, the measurements were also repeated on the polymeric substrate in a vertical position (Figure 11B, right).

TEST ON BIOCOLONIZED SAMPLES

Samples preparation

Lecce stone, a Miocenic, fine-grained, and generally mineralogically homogeneous pale yellow calcarenite, was selected for this study. It has an average porosity of 31.4%, with a pore size distribution evaluated with mercury intrusion porosimetry that ranges between 0.1 and 2.5 μm and an average pore diameter of 0.2 μm. The main mineralogical component is calcite, with a negligible fraction of silicates. This lithotype was selected because of its characteristic mineralogical and physical properties, which make it particularly suitable for laboratory colonization. Moreover, this stone has been extensively investigated in the scientific literature, and many reference studies providing data on its real-world response to biocolonization and weathering are available (see, for example,[40–43]). The two types of SABs, mono-species and dual-species, were grown on 5.0 cm × 5.0 cm x 1.0 cm specimens.

The protocol developed by Villa et al.[20] ensures strong biofilm adhesion and uniform surface coverage on natural stones, making these systems highly suitable for controlled and reproducible studies of microbial colonization. Moreover, their demonstrated ability to confer hydrophobic characteristics to surfaces, without completely preventing liquid water absorption, further enhances their suitability for studying surface modifications under realistic environmental conditions.[14,18]

Based on these premises, the following protocol was applied to cultivate the selected biofilm systems. Axenic cultures of the phototrophic bacterium were grown in BG11 medium.[44] The cultivation was carried out at room temperature in 250-mL Erlenmeyer flasks under daylight. Axenic cultures of *B. subtilis* NCIB 3610 were grown overnight in TSB (Tryptic Soy Broth) medium[45] at 30°C on an orbital shaker. Both biofilms were grown according to the protocol reported by Villa et al. (2015)[20] and modified as follows to obtain homogeneous coverage of the stone surface. The stone samples were immersed overnight in the planktonic culture composed of only cyanobacteria or the cyanobacteria and *B. subtilis* cellular suspensions in a 1:1 ratio. Then, the liquid culture was removed, and the samples were transferred into a glass Petri dish (Ø = 12 mm) on a filter paper pad 7 mm thick. The BG11 medium was added to wet the paper pad and maintained at 3 mm below the bottom of the paper pad. BG11 was also sprayed 3 times on the samples once a day in a vertical position and left to dry for a few minutes. After 7 days with a 16/8 days/night photoperiod, the SABs were mature, as already demonstrated by Villa et al.,[20] and the samples were ready for the test. Three samples for each type of biofilm were prepared. During the tests, the temperature and relative humidity values were monitored and were respectively 20.8°C ± 0.5 and 49.4% ± 2.6.

SAB architecture and characterization

Laboratory SABs grown on stone samples were studied by 3D optical microscopy, Scanning Electron Microscopy (SEM), and Confocal Laser Scanning Microscopy (CLSM). Moreover, cross-sections were prepared and analyzed to investigate biofilm thickness and endolithic growth.

The surface of biocolonized and uncolonized samples was analyzed to evaluate the biofilm surface coverage and to visualize and quantify the possible modification of surface texture due to the SAB's growth. A VHX-6000 digital microscope (KEYENCE, Itasca, IL, USA) with a 1/1.8-inch CMOS image sensor (1600 × 1200 pixels) was used. Images were acquired in three different areas of about (3.0 x 4.0) mm^2 of the analyzed surface. The magnification was 300x. The 3D Image stitching tool was used to obtain 3D images

by z stack composition of sequences of images collected at various focal depths, with vertical steps (z-steps) of about 50 mm. Roughness data (Ra and Rz) were then obtained by calculating the average values of 30 transects for each sample. Ra is defined as the arithmetical mean of all peak-valley heights of the assessed profile, while Rz is the sum of the vertical distances of the five highest (peaks) and the five deepest (valleys) values of the assessed profile.[46]

SEM images were acquired on Lecce stone fragments biocolonized with dual-species and mono-species SABs. Images were acquired on the ZEISS GeminiSEM 300 (ZEISS, Jena Germany) in high vacuum mode. The fragments were carbon-coated. A secondary electron detector and a voltage of 5 kV were used.

For the SABs architecture visualization, confocal images were collected using a Nikon A1/A1R confocal microscope (Nikon Instruments Inc., Amstelveen, Netherlands) and a 20x dry objective. A portion of each type of biofilm was stained using SYTO9 (Green Fluorescent Nucleic Acid Stain, ThermoFisher Scientific) to visualize *B. subtilis* NCIB 3610 cells, and Concanavaline A (ConA, Texas Red, ThermoFisher Scientific) to visualize the extracellular glycoconjugates, for the dual-species biofilm and only with ConA for the mono-species. According to the manufacturer's instructions, the samples were covered with SYTO9 and ConA or only ConA in water and incubated for 30 min in the dark at room temperature. After incubation, the samples were rinsed three times with water to remove any residual stains. Fluorescence was excited and collected using the following laser lines and emission parameters: for *B. subtilis* NCIB 3610 (SYTO9), ex 488 nm, em 500–550 nm, autofluorescence of *Synechocystis* sp. with ex 633 nm, and em 650–750 nm for the extracellular glycoconjugates of the EPS (ConA) ex 561 nm, em 570–620 nm. Images were captured and analyzed with the software Imaris (Bitplane Scientific Software, Switzerland) for 3D reconstructions of SABs. A minimum of five SAB areas for each type of biofilm (mono-species and dual-species) were analyzed. The images were also processed to quantify the proportion of red, green, and blue signals to calculate the associated biovolumes using ImageJ software.

Finally, polished cross-sections were prepared by embedding sample fragments in the Technovit 2000 LC Fixierpaste (Kulzer GmbH, Hanau, Germany). They were observed by means of a Leica DM6M optical microscope in dark-field mode, equipped with a Leica FLEXACAM C1 color digital camera.

Benchtop contact angle measurements

A Drop Shape Analyzer (A. KRÜSS Optronic, Hamburg, Germany) was used as described in 2.a. A 60-fps video of 15 s and 10 min was recorded respectively for uncolonized and biocolonized (mono- and dual-species biofilm) samples and elaborated *a posteriori*. After the drop stabilization on the surface (resulting in a stable and fully focused drop shape), the static water contact angle was calculated according to the Young-Laplace model. Drop absorbance times were calculated at complete absorption (loss of mirror effect). Measurements were repeated 15 times for each sample (45 drops in total for each type of biofilm).

Portable contact angle measurements

A Mobile Surface Analyzer instrument (A. KRÜSS Optronic, Hamburg, Germany) was used as described in 2.b. A 10-fps video of 15 s and 10 min was recorded respectively for uncolonized and biocolonized (mono- and dual-species biofilm) samples and elaborated *a posteriori*. After drop stabilization on the surface (resulting in a stable and fully focused drop shape), the static water contact angle was calculated for each drop according to the Young-Laplace model. The drop absorption time was calculated at complete absorption of the drop (loss of mirror effect). Measurements were repeated 15 times for each sample (45 drops in total for each type of biofilm).

QUANTIFICATION AND STATISTICAL ANALYSIS

Statistical variability analysis and sample size determination

The first problem addressed in the analysis was the sample size determination for targeted statistical precision in WCA measurement and drop volume measurement, both with benchtop and portable equipment. Addressing this problem is crucial for ensuring that the samples collected provide sufficient information to make reliable inferences about the unknown statistical population under study. In any experiment, selecting a sample size that balances the desired precision or confidence level with practical considerations like time and cost of data collection is crucial. When, as in our case, the population variability is unknown, it is useful to resort to resampling methods, such as bootstrapping – see for instance[47] for an example of the application procedure. This method involves randomly drawing samples with replacements from the original dataset to create multiple simulated datasets: for each resample of a given size, the statistic of interest, e.g., the mean, is recalculated, and the collection of outcomes is used to assess the variability of the statistics estimate from samples of that size. This allows for estimating the change in precision or confidence level as a function of the sample size. In this work, starting from a reference bootstrap population of 50 measurements collected with the portable instrument, we considered sample sizes $n = 4, 6, 8,$ and so on, up to 48. For each sample size n, we drafted 100,000 resamples, and for each resample, we identified the 2.5 and 97.5 percentiles to obtain the 95% confidence interval. Then we computed the percentage p of uncertainty over the mean value implied by these results and fitted the curve with an inverse square root of n function:

$$p(n) = b + a/\sqrt{n} \quad \text{(Equation 3)}$$

(this kind of dependence of the percentage error is expected due to the independence of the samples). Thanks to the inverse of the fitted function, one can compute the sample size required to achieve a target percentage error on the results.

Correlation between benchtop and portable measurement methods

The consistency between benchtop and portable measurements was assessed by comparing the WCA and absorption time results for different biocolonized samples, each representing a combination of factors (e.g., roughness, presence or not of biofilm, mono- or dual-species biofilm). Several data points, both for the WCA values and the absorption time, were collected under each combination of factors according to the two experimental setups; then the results were compared using a regression procedure. The quality of the regression was used to indicate the strength of the relationship between portable and benchtop measurements.

Statistical data analysis was conducted using the package JMP Pro 17.0.0 (jmp.com, accessed in September 2023), the statistical analysis platform R (within the environment RStudio), and the Python libraries scipy and sklearn.